

Antiproliferative and proapoptotic activity of GUT-70 mediated through potent inhibition of Hsp90 in mantle cell lymphoma

L Jin^{1,2}, Y Tabe^{*,1}, S Kimura³, Y Zhou¹, J Kuroda⁴, H Asou⁵, T Inaba⁵, M Konopleva⁶, M Andreeff⁷ and T Miida¹

¹Department of Clinical Laboratory Medicine, Juntendo University School of Medicine, 2-1-1 Hongo, Bunkyo-ku, Tokyo 113-8421, Japan; ²Sportology Center, Juntendo University School of Medicine, 2-1-1 Hongo, Bunkyo-ku, Tokyo 113-8421, Japan; ³Division of Hematology, Respiratory Medicine and Oncology, Department of Internal Medicine, Faculty of Medicine, Saga University, 5-1-1 Nabeshima, Saga 849-8501, Japan; ⁴Division of Hematology and Oncology, Department of Medicine, Kyoto Prefectural University of Medicine, 465 Kajii-cho, Kamigyo-ku, Kyoto 602-8566, Japan; ⁵Department of Molecular Oncology and Leukemia Program Project, Research Institute for Radiation Biology & Medicine, Hiroshima University, 1-2-3 Kasumi, Minami-ku, Hiroshima 734-8553, Japan; ⁶Department of Leukemia, The University of Texas MD Anderson Cancer Center, 1515 Holcombe Blvd., Houston, TX 77030, USA; ⁷Department of Stem Cell Transplantation and Cellular Therapy, The University of Texas MD Anderson Cancer Center, 1515 Holcombe Blvd., Houston, TX 77030, USA

BACKGROUND: Mantle cell lymphoma (MCL) is an aggressive B-cell lymphoma with poor prognosis, requiring novel anticancer strategies.

METHODS: Mantle cell lymphoma cell lines with known p53 status were treated with GUT-70, a tricyclic coumarin derived from *Calophyllum brasiliense*, and the biological and biochemical consequences of GUT-70 were studied.

RESULTS: GUT-70 markedly reduced cell proliferation/viability through G₁ cell cycle arrest and increased apoptosis, with greater sensitivity in mutant (mt)-p53-expressing MCL cells than in wild-type (wt)-p53-bearing cells. Mechanistically, GUT-70 showed binding affinity to heat-shock protein 90 (Hsp90) and ubiquitin-dependent proteasomal degradation of Hsp90 client proteins, including cyclin D1, Raf-1, Akt, and mt-p53. Depletion of constitutively overexpressed cyclin D1 by GUT-70 was accompanied by p27 accumulation and decreased Rb phosphorylation. GUT-70 induced mitochondrial apoptosis with Noxa upregulation and Mcl-1 downregulation in mt-p53 cells, but Mcl-1 accumulation in wt-p53 cells. Noxa and Mcl-1 were coimmunoprecipitated, and activated BAK. Treatment with a combination of GUT-70 and bortezomib or doxorubicin had synergistic antiproliferative effects in MCL cells that were independent of p53 status.

CONCLUSION: GUT-70 has pronounced antiproliferative effects in MCL with mt-p53, a known negative prognostic factor for MCL, through Hsp90 inhibition. These findings suggest that GUT-70 has potential utility for the treatment of MCL.

British Journal of Cancer (2011) **104**, 91–100. doi:10.1038/sj.bjc.6606007 www.bjancer.com

Published online 7 December 2010

© 2011 Cancer Research UK

Keywords: GUT-70; mantle cell lymphoma; apoptosis; p53; Hsp90; coumarin

Mantle cell lymphoma (MCL) is characterised by an aggressive clinical course, with rapid relapse after an initial response or primary resistance to standard chemotherapy (Jares *et al*, 2007). The t(11,14)(q13;32) translocation of MCL leads to overexpression of cyclin D1, which is believed to be associated with oncogenesis by causing instability of the G₁/S checkpoint through promotion of cyclin-dependent kinase activity and through sequestration of the Cip/Kip family of cyclin-dependent kinase inhibitors (Sherr and Roberts, 1999; Quintanilla-Martinez *et al*, 2003). These activities facilitate phosphorylation and inactivation of the retinoblastoma (Rb) G₁/S checkpoint protein, resulting in cell cycle progression. It has been demonstrated, however, that overexpression of cyclin D1 itself is not sufficient for development of MCL, suggesting that additional genetic events might be necessary for oncogenesis (Bodruga *et al*, 1994), particularly as apoptosis-related genes such

as p53, *INK4a/ARF*, and *ATM* are dysregulated in MCL (Fernández *et al*, 2005; Greiner *et al*, 2006).

In MCL, mutation/overexpression of p53 is reported as an adverse prognostic indicator (Jares *et al*, 2007). As many of the antitumour effects mediated by chemotherapeutic agents depend on a p53-related pathway, resistance to chemotherapy often develops through impaired p53 signalling (Döhner *et al*, 1995). The 26S proteasome inhibitor bortezomib retains activity in p53-mutant (mt-p53) cells and has demonstrated single-agent efficacy in relapsed or refractory MCL, which is, however, based mainly on prolonged response rather than on an increase in ultimate survival rate (Goy *et al*, 2009).

Therefore, development of novel compounds that target p53-independent signalling pathways is of considerable interest in the treatment of this disease.

We have reported that the newly discovered anticancer agent GUT-70, a natural product derived from the stem bark of *Calophyllum brasiliense*, demonstrated cytotoxic efficacy in human leukaemic cells (Kimura *et al*, 2005). GUT-70 (Figure 1), characterised as a tricyclic coumarin with the formula

*Correspondence: Dr Y Tabe; E-mail: tabe@juntendo.ac.jp

Revised 6 October 2010; accepted 22 October 2010; published online 7 December 2010

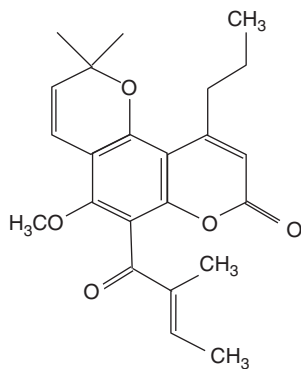


Figure 1 Chemical structure of GUT-70.

5-methoxy-2,2-dimethyl-6-(2-methyl-1-oxo-2-butenyl)-10-propyl-2H,8H-benzo[1,2-b;3,4-b']dipyran-8-one (C₂₃H₂₆O₅), significantly inhibited leukaemic cell growth with a median inhibitory concentration (IC₅₀) of 2–5 μM without repressing colony formation by normal haematopoietic progenitors or proliferation of normal human hepatocytes at concentrations up to 30 μM (Kimura *et al*, 2005).

Coumarin antibiotics have been reported to bind the newly discovered C-terminal ATP binding site of 90 kDa heat-shock protein (Hsp90), a molecular chaperone responsible for the folding and conformational maintenance of client proteins (Marcu *et al*, 2000; Issacs *et al*, 2003; Pratt and Toft, 2003; Donnelly *et al*, 2008). Hsp90 inhibition results in degradation of misfolded Hsp90 clients through ubiquitination, followed by proteasome-mediated hydrolysis (Zhang *et al*, 2004). As many of the Hsp90 client proteins contribute to cancer cell proliferation, Hsp90 has emerged as a promising target for cancer chemotherapy (Issacs *et al*, 2003; Donnelly *et al*, 2008).

In this study, GUT-70 demonstrated antiproliferative and proapoptotic activities with more prominent efficacy in mt-*p53*-bearing MCL cells than in those with wild-type (wt) *p53*. GUT-70 showed binding affinity to Hsp90, and reduced expression of Hsp90 client proteins such as mt-*p53*, Raf-1, cyclin D1, and Akt. The intrinsic apoptotic pathway was activated by GUT-70 through upregulation of Noxa and BAK activation. The combination of GUT-70 with bortezomib or doxorubicin yielded synergistic antiproliferative effects independent of *p53* status. These findings indicate possible efficacy and a rationale for further exploration of GUT-70 as a new therapeutic strategy for MCL.

MATERIALS AND METHODS

Cell lines and culture conditions

Four MCL cell lines were used in this study: JVM-2 (Melo *et al*, 1986), Granta 519 (Jadayel *et al*, 1997) and MINO (Lai *et al*, 2002) were kindly provided by Dr M Raffeld, and Jeko-1 (Raynaud *et al*, 1993) was a gift from Dr M Seto. Granta 519 and JVM-2 express wt-*p53*, whereas Jeko-1 and MINO express *p53* mutations (Jeko-1, loss of *p53* expression; MINO, mutation at codon 147 (valine → glycine)) (Raynaud *et al*, 1993; Lai *et al*, 2002). JVM-2, Jeko-1 and MINO were cultured in RPMI 1640 medium containing 15% fetal bovine serum (FBS) and 1% penicillin/streptomycin. Granta 519 was grown in Dulbecco's modified Eagle's medium (DMEM) supplemented with 15% FBS. Cells were first acclimated in RPMI 1640 or DMEM containing 5% FBS for 16 h before exposure to GUT-70 (Nippon Shinyaku, Kyoto, Japan) (Kimura *et al*, 2005). Control cells were treated with an equivalent amount of dimethyl sulphoxide (DMSO). Doxorubicin was obtained from Sigma

(St Louis, MO, USA) and bortezomib was provided by Millennium (Cambridge, MA, USA). Human osteosarcoma cell line U2OS transfected with the histone cluster 1 (*H2BK*) and enhanced green fluorescent protein (*EGFP*) genes, U2OS-H2BK-EGFP, was grown in DMEM supplemented with 10% FBS and used for morphological observation. U2OS expresses wt-*p53* (Flørenes *et al*, 1994).

Cell viability/proliferation assay

Cell viability was assessed by the Trypan blue dye exclusion method, and cell proliferation was determined by the CellTiter 96 Aqueous One Solution Cell Proliferation Assay (MTS; Promega, Madison, WI, USA).

Apoptosis analysis

Apoptotic cell death was evaluated through annexin V (Roche Diagnostic, Indianapolis, IN, USA) and propidium iodide (PI) positivities by a FACScan flow cytometer and Cell Quest software (Becton Dickinson Immunocytometry Systems, San Jose, CA, USA). The extent of drug-specific apoptosis was assessed by the following formula: % specific apoptosis = (test – control) × 100 / (100 – control).

Flow cytometric analysis of cell cycle and BAK activation

Cell cycle distribution was determined by flow cytometric analysis of PI-stained nuclei. DNA content was determined by FACScan flow cytometer and CellQuest software. BAK activation was analyzed as previously described (Samraj *et al*, 2006). Briefly, cells were fixed and permeabilized using the DAKO IntraStain kit (DakoCytomation, Glostrup, Denmark) according to the manufacturer's instructions. Cells were then stained with conformation-specific monoclonal antibody against BAK (y164; Abcam, Cambridge, MA, USA) or isotype-matched control antibody for 30 min at room temperature, followed by incubation with Alexafluor 488-labeled chicken anti-rabbit secondary antibody (Molecular Probes, Eugene, OR, USA) for 30 min on ice in the dark. After the washing step, conformational change of BAK was analyzed by a FACScan flow cytometer.

Western blot analysis and immunoprecipitation

Cells were solubilised in lysis buffer (phosphate-buffered saline solution (PBS), 1 × cell lysis buffer (Cell Signaling Technology, Danvers, MA, USA), 1 × protease inhibitor (Roche), and 1 × phosphatase inhibitor cocktails I and II (Calbiochem, San Diego, CA, USA)), and incubated for 30 min on ice. Total protein (20 μg) was separated by sodium dodecyl sulphate polyacrylamide gel electrophoresis (SDS-PAGE), immunoblotted with appropriate antibodies, and reacted with enhanced chemiluminescence reagent (Amersham Biosciences, Piscataway, NJ, USA); signals were detected by a luminescent image analyser (LAS-1000 plus; Fujifilm, Tokyo, Japan). The anti-α-tubulin or anti-β-actin blot was used in parallel as a loading control. For immunoblotting, the following antibodies were used: p21^{Cip1/WAF1}, p27^{KIP1}, and Mcl-1 (BD-Pharmingen, San Diego, CA, USA); p53 (DO-7; Dako, Carpinteria, CA, USA); Noxa (Calbiochem); α-tubulin (Sigma-Aldrich, St Louis, MO, USA); Puma (Upstate Biotechnology, Lake Placid, NY, USA); LC-3 (MBL, Nagoya, Japan); ubiquitin (Santa Cruz Biotechnology, Santa Cruz, CA, USA); and Hsp70, c-Raf, Akt, ERK1/2, phosphorylated-ERK1/2^{Thr202/Tyr204} (p-ERK1/2), cyclin D1, phosphorylated Rb^{Ser780} (p-Rb), Bim, BAK, cleaved caspase-9, cleaved caspase-3, β-actin, and horseradish peroxidase-linked anti-mouse and anti-rabbit IgG (all from Cell Signaling Technology). Protein lysates were subjected to immunoprecipitation using anti-Mcl-1 (Santa Cruz Biotechnology).

Hsp90 binding assay

The Hsp90 α inhibitor screening assay kit with Hsp90 α recombinant enzyme and fluorescein isothiocyanate (FITC)-labelled geldanamycin was used (BPS Bioscience, San Diego, CA, USA). The competition of fluorescence-labelled geldanamycin for binding to purified recombinant Hsp90 α was measured by Flex Station 3 (Molecular Devices, Sunnyvale, CA, USA).

Morphological observation

U2OS-H2BK-EGFP cells (2.0×10^5 per ml) were cultured in a 35-mm dish and treated with $5 \mu\text{M}$ GUT-70 or DMSO only. Each dish was placed on the stage of a light microscope equipped with a digital camera (BZ-8000; Keyence, Osaka, Japan) at 37°C under a

humidified atmosphere of 5% CO_2 . Video images were collected over the period from 12 to 48 h after treatment.

mRNA quantification by real-time reverse-transcriptase PCR (RT-PCR)

Total RNAs were extracted from cells with the RNeasy Mini Kit (Qiagen, Hilden, Germany). First-strand cDNA synthesis was performed with oligo(dT) as primer (Superscript II System; Invitrogen, Carlsbad, CA, USA). Real-time reverse-transcriptase PCR was performed by the Model 7500 Real-time PCR System (Applied Biosystems, Foster City, CA, USA). Expression of *Noxa* and *GAPDH* mRNA was detected by TaqMan Gene Expression Assays (*Noxa*: Hs00560402_m1, *GAPDH*: Hs99999905_m1; Applied Biosystems). The PCR cycle number that generated the first

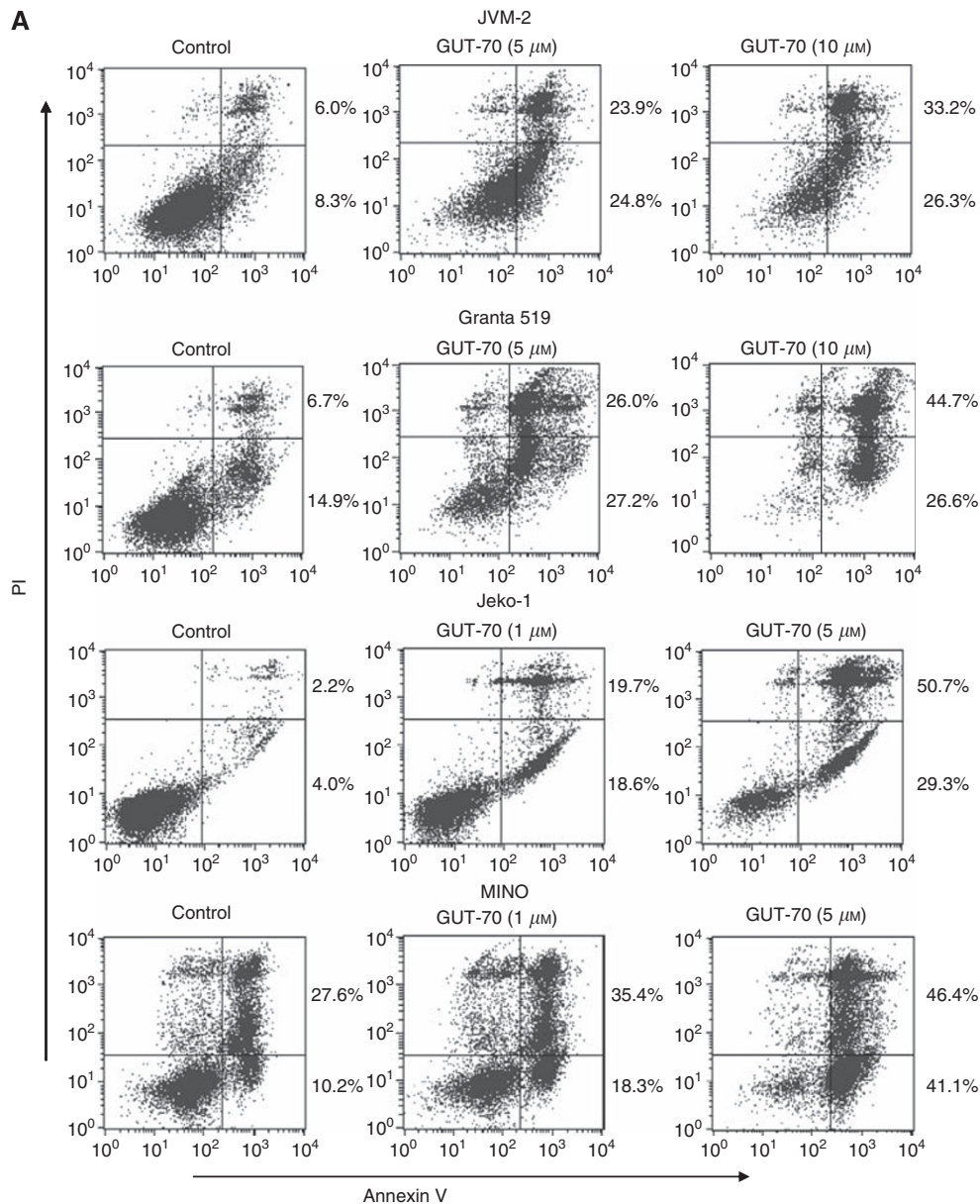


Figure 2 GUT-70-induced cell growth inhibition, apoptosis, and cell cycle arrest in MCL. **(A)** JVM-2, Granta 519, Jeko-1, and MINO cells were treated with the indicated concentrations of GUT-70 for 48 h, and the percentages of apoptotic cells were quantified by annexin V/PI staining. **(B)** Representative flow cytometric histograms of PI-treated cells after 24 h of GUT-70 treatment at indicated concentrations. The percentages of G_0/G_1 -, S- and G_2/M -phase cells were assessed in total viable cells (bar graphs).

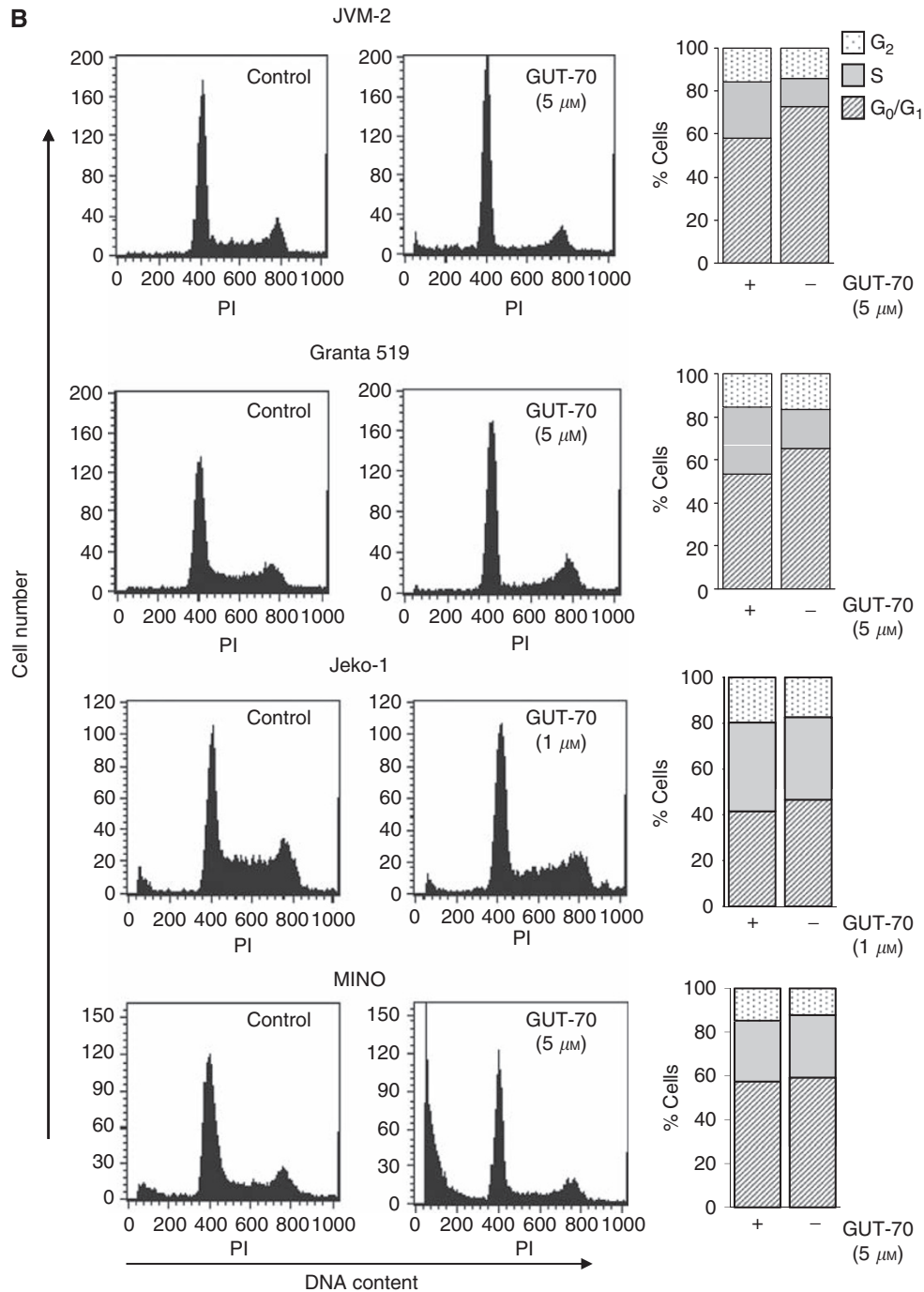


Figure 2 Continued.

fluorescence signal above a threshold value (the threshold cycle; C_t) was determined. The abundance of each transcript of *Noxa* relative to that of *GAPDH* was calculated as follows: relative expression = $100 \times 2^{-\Delta C_t}$, where ΔC_t is the mean C_t of the transcript of interest minus the mean C_t of the transcript for *GAPDH*. The C_t data from duplicate PCRs were averaged for calculation of relative expression.

Statistical analysis

Cytotoxicity was assessed by the Chou-Talalay method (Chou and Talalay, 1984) using Calcsyn software (Biosoft, Cambridge, UK). The combination index (CI) values indicate degree of synergism:

strong synergism (0.3–0.7), moderate synergism (0.7–0.85), and slight synergism (0.85–0.9).

RESULTS

GUT-70 induces apoptosis and cell cycle arrest in MCL cells

Treatment with GUT-70 (Figure 1) for 48 h resulted in dose-dependent cell growth inhibition detected by MTS cell proliferation assay (IC_{50} : Granta 519, 6.3 μM ; JVM-2, 4.5 μM ; Jeko-1, 1.7 μM ; MINO, 1.5 μM).

To determine whether the inhibition of cell growth by GUT-70 was associated with apoptosis and/or cell cycle arrest, we

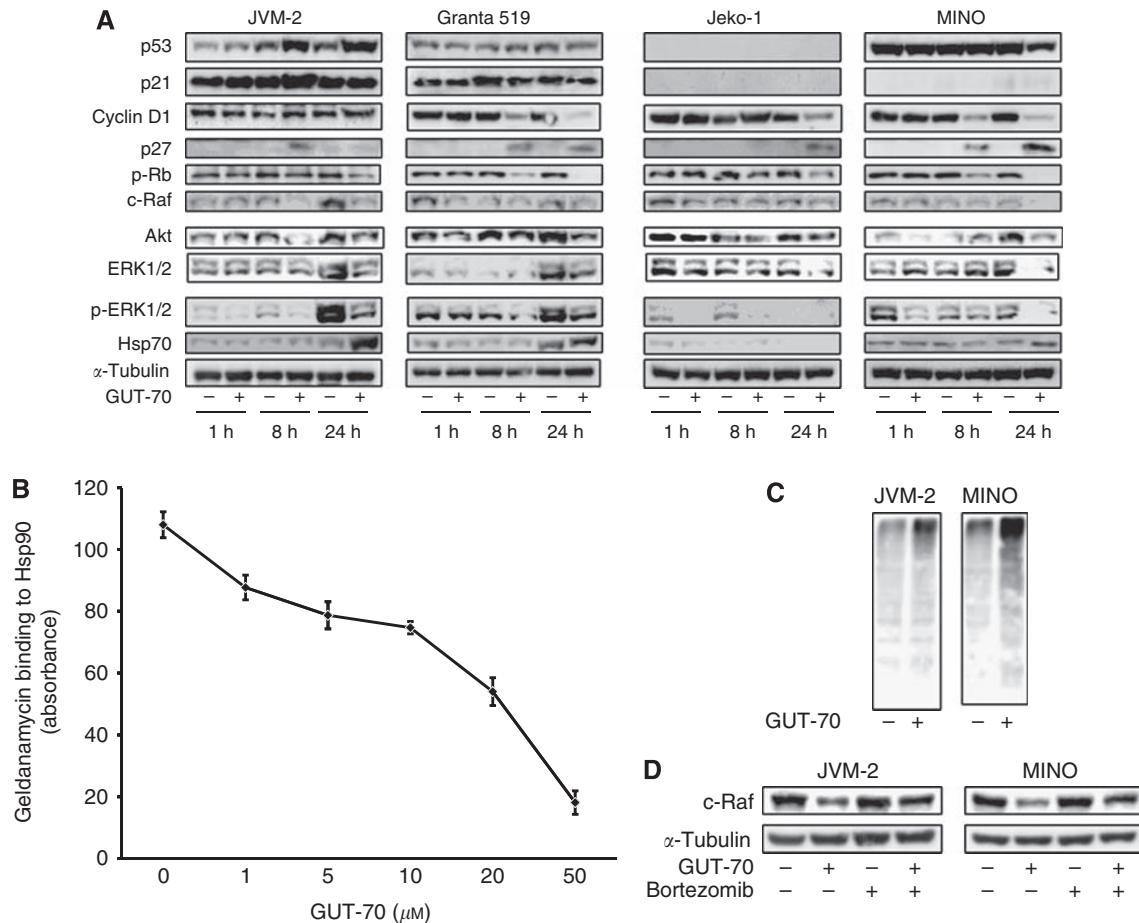


Figure 3 (A) GUT-70 effects on Hsp90 client proteins. MCL cells were treated with GUT-70 (JVM-2, 5 μM ; Granta 519, 5 μM ; Jeko-1, 1 μM ; MINO, 5 μM) for indicated times. Cells were subjected to lysis and analysed by western blot. Western blot images are representative results from three independent experiments. (B) GUT-70 competitively inhibited geldanamycin binding to the Hsp90 α subunit. The competition of GUT-70 with FITC-labelled geldanamycin for binding to purified recombinant Hsp90 α was measured. Fluorescence was measured at λ_{ex} 485 nm and at λ_{em} 525 nm. Results shown are means \pm s.d. from three independent experiments. (C) GUT-70 induced protein ubiquitination. JVM-2 and MINO cells were treated with 5 μM GUT-70 for 24 h, subjected to lysis, and immunoblotted for ubiquitin. Representative results are shown from three independent experiments. (D) Proteasome inhibitor bortezomib prevented GUT-70-mediated decreased expression of c-Raf. JVM-2 and MINO cells were treated with 5 μM GUT-70 and/or 10 nM bortezomib for 24 h, subjected to lysis, and immunoblotted for c-Raf. Western blot images are representative results from three independent experiments.

conducted flow cytometric analysis of annexin V/PI-stained and PI-stained nuclei. As shown in Figure 2A, 48 h of GUT-70 treatment induced dose-dependent increases of annexin V positivity in all cell lines; this effect was more pronounced in mt-*p53*-bearing Jeko-1 and MINO cells than in wt-*p53*-bearing Granta 519 and JVM-2 cells (specific apoptosis by 5 μM GUT-70: 40.3% for Granta 519, 40.1% for JVM-2, 78.8% for Jeko-1, 79.9% for MINO). The PI cell cycle histograms further demonstrated that GUT-70 increased the sub- G_1 fraction in a time-dependent manner at a lower dose for mt-*p53* cells than for wt-*p53* cells; sub- G_1 fractions at 24 and 48 h were 4.6 and 10.7% for Granta 519 (5 μM GUT-70), 14.8 and 34.7% for JVM-2 (5 μM), 5.2 and 19.3% for Jeko-1 (1 μM), and 12.0 and 34.9% for MINO (1 μM). Whereas GUT-70 impeded G_1 -S cell cycle progression in JVM-2 and Granta 519 cells, G_1 -S arrest was minimal in MINO and Jeko-1 cells (Figure 2B). These data suggest that GUT-70-induced cell growth inhibition resulted in part from cell cycle arrest at the G_0/G_1 checkpoint and in part from apoptosis induction.

GUT-70 downregulates mutated p53 and cyclin D1 and accumulates p27

We next investigated changes in cell cycle regulatory proteins associated with GUT-70 treatment. As shown in Figure 3A, GUT-70

induced p53/p21 accumulation in JVM-2 cells, but did not increase p53/p21 expression in Granta 519 cells. In Jeko-1 cells, basal p53/p21 expression was not detectable and was unaffected by GUT-70. Notably, expression of the overexpressed mt-p53 protein was reduced in MINO cells by 24 h exposure to GUT-70, without detectable p21 expression. The expression level of p27 was upregulated by GUT-70, irrespective of *p53* status. GUT-70 diminished the highly expressed cyclin D1 in all tested MCL cells except JVM-2, and resulted in substantial decreases in Rb phosphorylation in all tested cells (Figure 3).

GUT-70 induces degradation of Hsp90 substrate proteins

The coumarin antibiotics have been reported to bind to Hsp90 (Marcu *et al*, 2000). To investigate whether GUT-70 has binding affinity for Hsp90, a competitive binding assay was performed using geldanamycin, a well-characterised ATP competitive inhibitor (Gooljarsingh *et al*, 2006). GUT-70 demonstrated dose-dependent inhibition of geldanamycin binding to Hsp90, which indicated the binding activity of GUT-70 to Hsp90 (Figure 3B). The degradation by GUT-70 of Hsp90 client proteins, such as Raf-1 and its downstream ERK1/2 and phospho ERK1/2, as well as Akt (Pratt and Toft, 2003; Zhang *et al*, 2004, 2005), was detected by

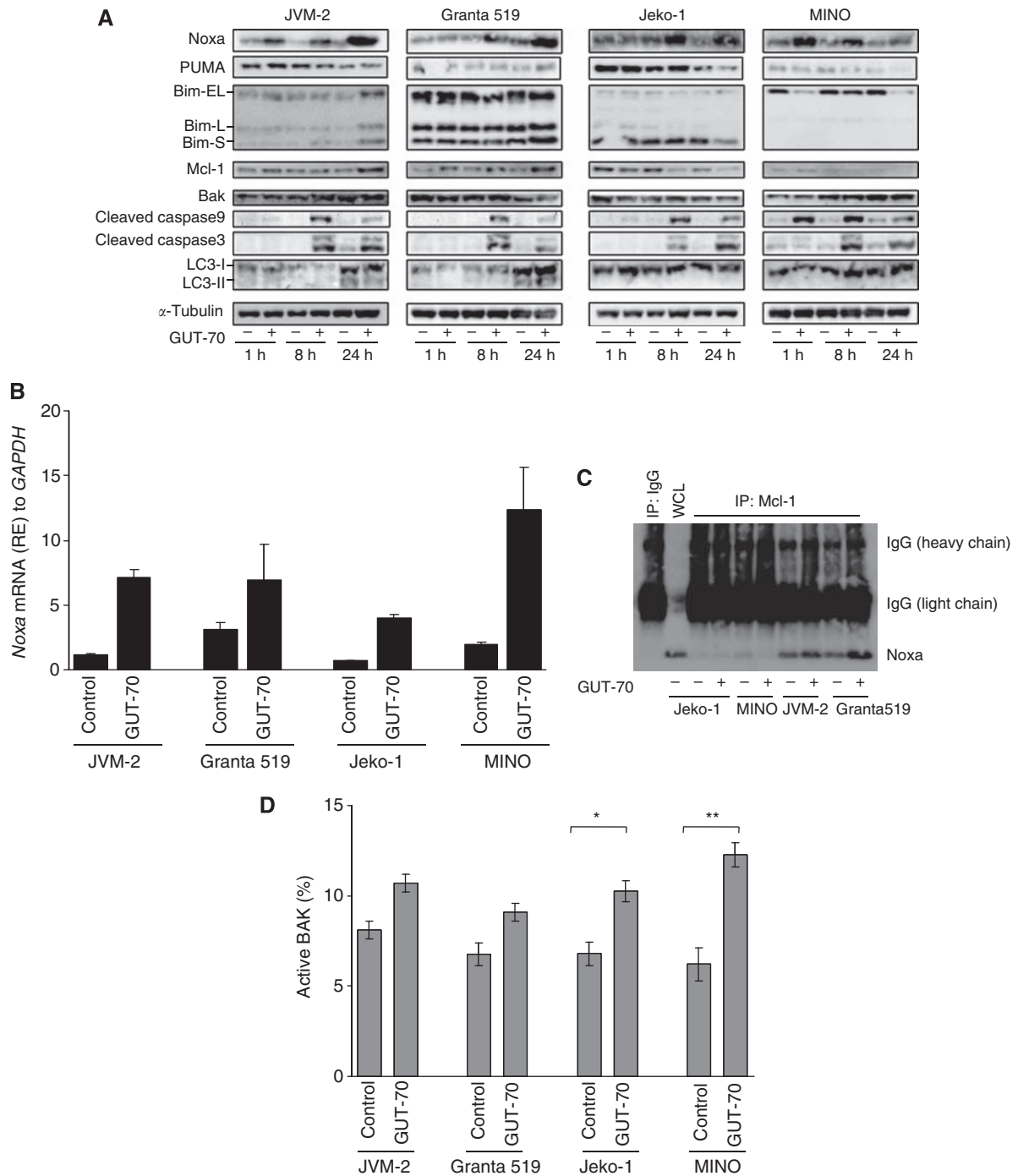


Figure 4 Modulation of apoptosis-related protein levels by GUT-70. MCL cells were treated with GUT-70 (JVM-2, 5 μ M; Granta 519, 5 μ M; Jeko-1, 1 μ M; MINO, 5 μ M) for the indicated times. **(A)** Cells were subjected to lysis, then apoptosis-related proteins and macroautophagy marker LC3 were analysed by western blot. Western blot images are representative results from three independent experiments. **(B)** Cells were harvested after 18 h treatment with GUT-70, and *Noxa* mRNA expression levels were detected by TaqMan RT-PCR analysis. The abundance of transcripts of *Noxa* relative to *GAPDH* transcripts was determined as described in Materials and Methods. Graphs show the representative data from two independent experiments with similar results. **(C)** Cells were treated with GUT-70 for 24 h, and Mcl-1 immunoprecipitation was performed as described in Materials and Methods. Total extracts were analysed by western blotting for Noxa. Western blot images are representative results from three independent experiments. **(D)** Cells were treated with GUT-70 for 24 h, then conformational changes in BAK were measured by intracellular flow cytometry as described in Materials and methods. To block the caspase activation-mediated conformational changes of BAK, cells were preincubated for 1 h with 100 μ M Z-VAD-FMK. Data represent duplicate experiments. * $P < 0.01$; ** $P < 0.05$. RE, relative expression.

western blot analysis in all tested MCL cells (Figure 3A). Cyclin D1 and mt-p53, the expression of which was repressed by GUT-70, are known substrate proteins of Hsp90 (Zhang *et al*, 2004; Muller *et al*, 2008). Furthermore, GUT-70 increased expression of Hsp70, a

marker of Hsp90 inhibition (Elo *et al*, 2005; Bao *et al*, 2009), in Granta 519, JVM-2, and MINO cells. In Jeko-1 cells, however, Hsp70 was detected at a level insufficient to be reliable as a marker without further induction by GUT-70 (Figure 3A).

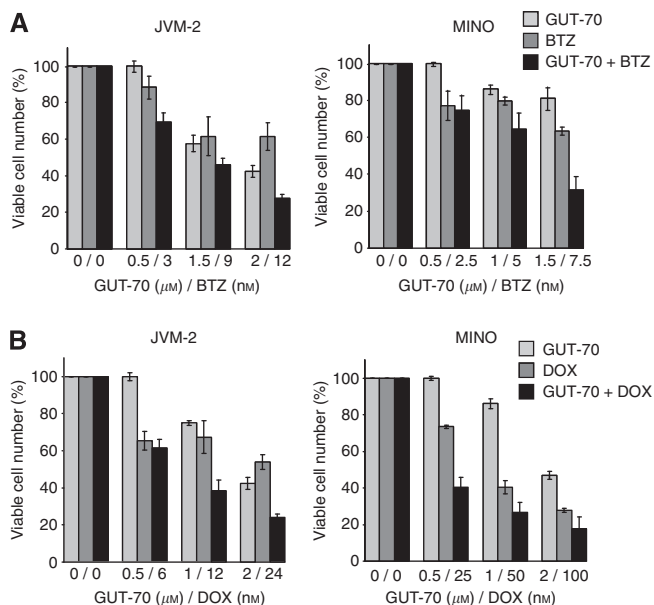


Figure 5 Synergistic interaction between GUT-70 and bortezomib or doxorubicin in MCL cells. JVM2 and MINO cells were cultured in the presence of escalating doses of GUT-70 and bortezomib (BTZ) (**A**) or GUT-70 and doxorubicin (DOX) (**B**) at a fixed ratio. After 48 h, viable and dead cells were identified using the Trypan blue dye exclusion method. Results are expressed as means \pm s.d. percentage of viable cell numbers in control cells.

As the client proteins of Hsp90 chaperone molecule become misfolded and ubiquitinated by Hsp90 inhibition, and are then downregulated by proteasomal degradation (Issacs *et al*, 2003; Zhang *et al*, 2004), we next tried to determine whether GUT-70 induces protein ubiquitination followed by proteasomal degradation in wt-*p53*-expressing JVM-2 and mt-*p53*-expressing MINO cells. As expected, GUT-70 treatment elevated the level of protein ubiquitination (Figure 3C); subsequent treatment with proteasome inhibitor bortezomib prevented degradation of c-Raf by GUT-70 (Figure 3D). Taken together, these data indicate the interaction of GUT-70 with Hsp90 and the destabilisation of Hsp90 client proteins by GUT-70.

Effect of GUT-70 on apoptosis-related proteins

To characterise the mechanism of GUT-70-induced cell death in MCL cells, we analysed the expression of apoptosis-related Bcl-2 family proteins, the BH3-only proteins Noxa, Puma, and Bim, and the other Bcl-2 family proteins, Mcl-1 and BAK, in MCL cell lines. Results show that GUT-70 induced substantial accumulation of Noxa but not of Puma (Figure 4A). Mutant-*p53*-bearing MCL cells demonstrated earlier Noxa induction than wt-*p53* cells; peak induction of Noxa was observed after 1 h of GUT-70 treatment in MINO, after 8 h in Jeko-1, and after 24 h in JVM-2 and Granta 519 cells. GUT-70 induced upregulation of Noxa mRNA levels in all tested cells (Figure 4B).

After 24 h of GUT-70 treatment, levels of antiapoptotic protein Mcl-1 were increased in JVM-2 and Granta 519 cells, but decreased in Jeko-1 and MINO cells (Figure 4A). It is known that Noxa binds preferentially to Mcl-1 (Warr and Shore, 2008), triggers BAK or Bim release from Mcl-1, and then starts the mitochondrial apoptotic pathway (Willis *et al*, 2005; Hauck *et al*, 2009). Concomitantly, we detected coimmunoprecipitation between Noxa and Mcl-1 (Figure 4C) in JVM-2 and Granta 519 cells, both of which showed accumulation of Mcl-1 induced by GUT-70. Although total

BAK expression levels remained, consistently independent of GUT-70 treatment (Figure 4A), flow cytometric analysis revealed a pronounced increase of activated BAK in MINO, moderate activation in Jeko-1, and only slight activation in JVM-2 and Granta 519 cells after GUT-70 treatment (Figure 4D), activities that are in inverse relation to Mcl-1 expression levels.

Proapoptotic BH-3-only protein Bim was induced by GUT-70 at 24 h in JVM-2 cells but not in the other cell lines (Figure 4A).

GUT-70 does not induce macroautophagy

Increasing evidence indicates that autophagy is one of the important mechanisms of anticancer reagent-induced cell death (Tsujimoto and Shimizu, 2005). In mammals, three modes of autophagy have been identified: macroautophagy, microautophagy, and chaperone-mediated autophagy (Levine and Klionsky, 2004). To investigate the possibility that GUT-70 promotes macroautophagy, we examined the conversion of light chain 3 (LC3) from LC3-I to LC3-II, a marker of autophagosome formation (Kabeya *et al*, 2000). Whereas LC3-II was moderately induced by a low serum culture condition (5%, 40 h) in wt-*p53*-expressing JVM-2 and Granta 519 cells, there was no change in accumulation of LC3-II following further treatment with GUT-70 (24 h). In mt-*p53*-bearing MINO and Jeko-1 cells, neither serum starvation nor GUT-70 treatment induced LC3-II accumulation (Figure 4A).

To assess the morphological changes induced by GUT-70, U2OS-H2BK-EGFP cells were sequentially photographed after exposure to GUT-70. Cells underwent morphological alterations, including cytoplasmic swelling and vacuolisation after 24 h of GUT-70 exposure (cellular oncosis), and cell death peaked at 36 h (secondary necrosis) (Supplementary Material 1 for Quick-Time movies) (Majno and Joris, 1995; Lemasters *et al*, 1998; Van Cruchten and Van Den Broeck, 2002).

Combination of GUT-70 with bortezomib or doxorubicin has synergistic effects on MCL growth inhibition

To determine whether GUT-70 potentiates the commonly used chemotherapeutic agents, we assessed the effects of combinations of GUT-70 with bortezomib, a selective inhibitor of the 26S proteasome, or doxorubicin, a conventional chemodrug for MCL, on viability of wt-*p53* JVM-2 and mt-*p53* MINO cells. As shown in Figure 5A, both of these combination treatments had observable synergistic effects in both cell types 48 h after exposure. The averaged CI values of GUT-70/bortezomib treatment were 0.59 for JVM2 and 0.73 for MINO; for GUT-70/doxorubicin, 0.37 for JVM2 and 0.35 for MINO, indicating strong and moderate synergism, respectively.

DISCUSSION

The natural product-derived tricyclic coumarin GUT-70 exhibited single-agent antiproliferative and proapoptotic activities against MCL cell lines as a novel Hsp90 inhibitor. GUT-70's dose-dependent inhibition of geldanamycin binding to Hsp90 α indicates that GUT-70 has direct binding activity to Hsp90, by which GUT-70 induces conformational change in the Hsp90 molecule and interferes with its binding of geldanamycin. This finding agrees with that of previous studies showing that coumarin antibiotic novobiocin binds to the Hsp90 C-terminal ATP binding site and affects the binding of geldanamycin at the Hsp90 N-terminal domain through close interaction between amino and carboxy termini in solution (Csermely *et al*, 1998; Hartson *et al*, 1999; Marcu *et al*, 2000; Donnelly *et al*, 2008). GUT-70 induced depletion of Hsp90 client proteins mt-*p53*, Raf-1, cyclin D1, and Akt, and increased Hsp70, a marker of Hsp90 inhibition; these findings, along with the ubiquitin-dependent proteasomal degradation of

Hsp90 client proteins, suggest that GUT-70 functions as an Hsp90 inhibitor.

It is important that mt-*p53*-expressing MCL cells were more sensitive to GUT-70-induced apoptosis than wt-*p53*-bearing MCL cells. In mt-*p53* cells, prominent GUT-70-induced apoptosis was accompanied by minimal cell cycle arrest, which is consistent with a previous report of G₂/M checkpoint abrogation in p53/p21-impaired cells through downregulation of Chk1 and Wee1 by Hsp90 inhibitor that resulted in premature mitotic entry and mitotic death (Tse *et al*, 2009).

Furthermore, GUT-70 induced the most pronounced apoptosis in MINO cells in which GUT-70 treatment depleted overexpressed mt-*p53*. mt-*p53* is known to confer the additional 'gain of function' as the transcription regulator. Transcriptional activation by mt-*p53* has been reported for *MDR1* (Sampath *et al*, 2006), *c-MYC* (Frazier *et al*, 1998), or *GRO1* (Yan and Chen, 2009), resulting in cell proliferation, antiapoptosis, and tumorigenicity (Blandino *et al*, 1999). GUT-70-induced degradation of mt-*p53* may successfully repress these oncogenic transcriptional activations.

Another important finding of this study is the prominent p53-independent Noxa upregulation by GUT-70. Whereas Noxa had been proposed to be a critical mediator of p53-dependent apoptosis (Oda *et al*, 2000), p53-independent upregulation of Noxa has been described in MCL and B-cell chronic lymphocytic leukaemia (Pérez-Galán *et al*, 2006; Smit *et al*, 2007). Furthermore, GUT-70 induced Noxa protein accumulation extremely early (1 h) in mt-*p53*-bearing MINO cells, indicating independence from transcriptional gene induction. Recently, Noxa degradation by direct interaction with a spliced isoform of the Kruppel-like tumour suppressor (KLF6-SV1) (Difeo *et al*, 2009), or by posttranscriptional stabilisation/destabilisation of *Bim* mRNA (Matsui *et al*, 2007), has been reported. Our findings indicate the possibility of posttranscriptional Noxa stabilisation by GUT-70, which requires further elucidation.

The preferred binding partner of Noxa is the multidomain antiapoptotic Bcl-2 family member Mcl-1. In response to apoptotic stimuli, Noxa binds to Mcl-1, which ultimately leads to activation of BAK by releasing BAK from the BAK-Mcl-1 complex, and triggers BAK-mediated cell death (Chen *et al*, 2005; Warr and Shore, 2008) (Figure S, Supplementary Material 2 (Kuroda and Kimura, 2007)). The balance between Noxa and Mcl-1 is proposed to determine cell fate as death versus survival (Mei *et al*, 2007). GUT-70-induced BAK activation and sequential apoptosis were associated with Mcl-1 accumulation levels; high levels in less-sensitive wt-*p53* cells and low levels in highly sensitive mt-*p53* cells were consistent with previous reports (Pérez-Galán *et al*, 2006; Mei *et al*, 2007).

Autophagy is known to promote both autophagic cell death and cell survival (Kamitsui *et al*, 2008). Although GUT-70 did not affect autophagosome formation, Hsp90 clients have been shown to be degraded through chaperone-mediated autophagy (Shen *et al*, 2009). The role of GUT-70 in induction of chaperone-mediated autophagy requires further elucidation.

The observed morphological changes in GUT-70-treated cells (e.g., swelling cytoplasm) indicate cellular oncosis (Van Cruchten

and Van Den Broeck, 2002), which shares certain mechanisms and alterations with apoptosis, such as loss of mitochondrial permeability and membrane potential (Lemasters *et al*, 1998).

Furthermore, our results demonstrate that GUT-70 can synergise the cytotoxic effects of the proteasome inhibitor bortezomib and the widely used genotoxic chemotherapeutic agent doxorubicin in MCL cells (Brody and Advani, 2006; Goy *et al*, 2009), regardless of p53 status. Previously, a combination of Hsp90 inhibitor geldanamycin and bortezomib was demonstrated to simultaneously disrupt Hsp90 and proteasome function, promote accumulation of ubiquitinated proteins, and enhance antitumour activity in human breast cancer cells (Mimnaugh *et al*, 2004, 2006). Whereas bortezomib induces longer-term remission (Goy *et al*, 2009), patients ultimately succumb to the poor clinical outcome, and there is a critical need to develop the most effective combination. The synergistic effects of GUT-70 and bortezomib may offer more efficacy and flexibility to the treatment of MCL with bortezomib. The antiproliferative effect of the combination of doxorubicin and GUT-70 was consistent with the previous findings for doxorubicin and Hsp-90 inhibitor 17-(dimethylaminoethylamino)-17-demethoxygeldamycin (DMAG), which induced premature mitosis, followed by apoptosis, by bypassing the G₂/M checkpoint in lymphoma cells (Robles *et al*, 2006). The synergy with doxorubicin suggests that addition of GUT-70 may allow reduction in the therapeutic dose of doxorubicin, which could potentially reduce its genotoxic side effects (Brody and Advani, 2006). A development of *in vivo* studies of these combination treatments for MCL is further required.

In conclusion, our results demonstrate that the novel anticancer agent GUT-70, a tricyclic coumarin, inhibits cell proliferation by depleting Hsp90 substrates cyclin D1, Akt, and Raf-1, and induces mitochondrial apoptotic cell death with upregulation of Noxa in MCL cells. Notably, these effects are substantially pronounced in MCL cells with mt-*p53*, a known negative prognostic factor for MCL. These findings suggest that GUT-70 has potential utility for the treatment of MCL.

ACKNOWLEDGEMENTS

We thank Drs Kazuhisa Iwabuchi and Akimasa Someya for invaluable help and discussion; Tomomi Ikeda and Takako Shigihara-Ikegami for technical assistance; and Drs Mark Raffeld and Masao Seto for the gifts of cell lines. We thank Katy Hale for manuscript review. This work was supported by the Project Research Program of Juntendo University School of Medicine (to LJ), the Japan Leukemia Research Fund (to YT) and the Research for Promoting Technological Seeds of the Japan Science and Technology Agency (to SK).

Supplementary Information accompanies the paper on British Journal of Cancer website (<http://www.nature.com/bjc>)

REFERENCES

- Bao R, Lai CJ, Qu H, Wang D, Yin L, Zifcak B, Atoyian R, Wang J, Samson M, Forrester J, DellaRocca S, Xu GX, Tao X, Zhai HX, Cai X, Qian C (2009) CUDC-305, a novel synthetic HSP90 inhibitor with unique pharmacologic properties for cancer therapy. *Clin Cancer Res* 15: 4046–4057
- Blandino G, Levine AJ, Oren M (1999) Mutant p53 gain of function: differential effects of different p53 mutants on resistance of cultured cells to chemotherapy. *Oncogene* 18: 477–485
- Bodrug SE, Warner BJ, Bath ML, Lindeman GJ, Harris AW, Adams JM (1994) Cyclin D1 transgene impedes lymphocyte maturation and collaborates in lymphomagenesis with the *myc* gene. *EMBO J* 13: 2124–2130
- Brody J, Advani R (2006) Treatment of mantle cell lymphoma: current approach and future directions. *Crit Rev Oncol Hematol* 58: 257–265
- Chen L, Willis SN, Wei A, Smith BJ, Fletcher JI, Hinds MG, Colman PM, Day CL, Adams JM, Huang DC (2005) Differential targeting of pro-survival Bcl-2 proteins by their BH3-only ligands allows complementary apoptotic function. *Mol Cell* 17: 393–403
- Chou TC, Talalay P (1984) Quantitative analysis of dose-effect relationships: the combined effects of multiple drugs or enzyme inhibitors. *Adv Enzyme Regul* 22: 27–55

- Csermely P, Schnaider T, Soti C, Prohaszka Z, Nardai G (1998) The 90-kDa molecular chaperone family: structure, function, and clinical applications. A comprehensive review. *Pharmacol Ther* 79: 129–168
- Difeo A, Huang F, Sangodkar J, Terzo EA, Leake D, Narla G, Martignetti JA (2009) KLF6-SV1 is a novel antiapoptotic protein that targets the BH3-only protein NOXA for degradation and whose inhibition extends survival in an ovarian cancer model. *Cancer Res* 69: 4733–4741
- Döhner H, Fischer K, Bentz M, Hansen K, Benner A, Cabot G, Diehl D, Schlenk R, Coy J, Stilgenbauer S, Volkman M, Galle PR, Poustka A, Hunstein W, Lichter P (1995) p53 gene deletion predicts for poor survival and non-response to therapy with purine analogs in chronic B-cell leukemias. *Blood* 85: 1580–1589
- Donnelly AC, Mays JR, Burlison JA, Nelson JT, Vielhauer G, Holzbeierlein J, Blagg BS (2008) The design, synthesis, and evaluation of coumarin ring derivatives of the novobiocin scaffold that exhibit antiproliferative activity. *J Org Chem* 73: 8901–8920
- Elo MA, Kaarniranta K, Helminen HJ, Lammi MJ (2005) Hsp90 inhibitor geldanamycin increases hsp70 mRNA stabilisation but fails to activate HSF1 in cells exposed to hydrostatic pressure. *Biochim Biophys Acta* 1743: 115–119
- Fernández V, Hartmann E, Ott G, Campo E, Rosenwald A (2005) Pathogenesis of mantle-cell lymphoma: all oncogenic roads lead to dysregulation of cell cycle and DNA damage response pathways. *J Clin Oncol* 23: 6364–6369
- Flørenes VA, Maelandsmo GM, Forus A, Andreassen A, Myklebost O, Fodstad O (1994) MDM2 gene amplification and transcript levels in human sarcomas: relationship to TP53 gene status. *J Natl Cancer Inst* 86: 1297–1302
- Frazier MW, He X, Wang J, Gu Z, Cleveland JL, Zambetti GP (1998) Activation of c-myc gene expression by tumor-derived p53 mutants requires a discrete C-terminal domain. *Mol Cell Biol* 18: 3735–3743
- Gooljarsingh LT, Fernandes C, Yan K, Zhang H, Grooms M, Johanson K, Sinnamon RH, Kirkpatrick RB, Kerrigan J, Lewis T, Arnone M, King AJ, Lai Z, Copeland RA, Tummino PJ (2006) A biochemical rationale for the anticancer effects of Hsp90 inhibitors: slow, tight binding inhibition by geldanamycin and its analogues. *Proc Natl Acad Sci USA* 103: 7625–7630
- Goy A, Bernstein SH, Kahl BS, Djulbegovic B, Robertson MJ, de Vos S, Epper E, Krishnan A, Leonard JP, Lonial S, Nasta S, O'Connor OA, Shi H, Borral AL, Fisher RI (2009) Bortezomib in patients with relapsed or refractory mantle cell lymphoma: updated time-to-event analyses of the multicenter phase 2 PINNACLE study. *Ann Oncol* 20: 520–525
- Greiner TC, Dasgupta C, Ho VV, Weisenburger DD, Smith LM, Lynch JC, Vose JM, Fu K, Armitage JO, Brazziel RM, Campo E, Delabie J, Gascoyne RD, Jaffe ES, Muller-Hermelink HK, Ott G, Rosenwald A, Staudt LM, Im MY, Karaman MW, Pike BL, Chan WC, Hacia JG (2006) Mutation and genomic deletion status of ataxia telangiectasia mutated (*ATM*) and *p53* confer specific gene expression profiles in mantle cell lymphoma. *Proc Natl Acad Sci USA* 103: 2352–2357
- Hartson SD, Thulasiraman V, Huang W, Whitesell L, Matts RL (1999) Molybdate inhibits Hsp90, induces structural changes in its C-terminal domain, and alters its interactions with substrates. *Biochemistry* 38: 3837–3849
- Hauk P, Chao BH, Litz J, Krystal GW (2009) Alterations in the Noxa/Mcl-1 axis determine sensitivity of small cell lung cancer to the BH3 mimetic ABT-737. *Mol Cancer Ther* 8: 883–892
- Issacs JS, Xu W, Neckers L (2003) Heat shock protein 90 as a molecular target for cancer therapeutics. *Cancer Cell* 3: 213–217
- Jadayel DM, Lukas J, Nacheva E, Bartkova J, Stranks G, De Schouwer PJ, Lens D, Bartek J, Dyer MJ, Kruger AR, Catovsky D (1997) Potential role for concurrent abnormalities of the cyclin D1, *p16CDKN2* and *p15CDKN2B* genes in certain B-cell non-Hodgkin's lymphomas: functional studies in a cell line (Granta 519). *Leukemia* 11: 64–72
- Jares P, Colomer D, Campo E (2007) Genetic and molecular pathogenesis of mantle cell lymphoma: perspectives for new targeted therapeutics. *Nat Rev Cancer* 7: 750–762
- Kabeya Y, Mizushima N, Ueno T, Yamamoto A, Kirisako T, Noda T, Kominami E, Ohsumi Y, Yoshimori T (2000) LC3, a mammalian homologue of yeast Apg8p, is localized in autophagosome membranes after processing. *EMBO J* 19: 5720–5728
- Kamitsuji Y, Kuroda J, Kimura S, Toyokuni S, Watanabe K, Ashihara E, Tanaka H, Yui Y, Watanabe M, Matsubara H, Mizushima Y, Hiraumi Y, Kawata E, Yoshikawa T, Maekawa T, Nakahata T, Adachi S (2008) The Bcr-Abl kinase inhibitor INNO-406 induces autophagy and different modes of cell death execution in Bcr-Abl-positive leukemias. *Cell Death Differ* 15: 1712–1722
- Kimura S, Ito C, Jyoko N, Segawa H, Kuroda J, Okada M, Adachi S, Nakahata T, Yuasa T, Filho VC, Furukawa H, Maekawa T (2005) Inhibition of leukemic cell growth by a novel anti-cancer drug (GUT-70) from *Calophyllum brasiliense* that acts by induction of apoptosis. *Int J Cancer* 113: 158–165
- Kuroda J, Kimura S (2007) The role of BH3-only proteins in cancer and anti-cancer therapeutics. *Cell Apoptosis Research Trends*. In Zhang CV (ed) pp 1–39. Nova: New York
- Lai R, McDonnell TJ, O'Connor SL, Medeiros LJ, Oudat R, Keating M, Morgan MB, Curiel TJ, Ford RJ (2002) Establishment and characterization of a new mantle cell lymphoma cell line, MINO. *Leuk Res* 26: 849–855
- Lemasters JJ, Nieminen AL, Qian T, Trost LC, Elmore SP, Nishimura Y, Crowe RA, Cascio WE, Bradham CA, Brenner DA, Herman B (1998) The mitochondrial permeability transition in cell death: a common mechanism in necrosis, apoptosis and autophagy. *Biochim Biophys Acta* 1366: 177–196
- Levine B, Klionsky DJ (2004) Development by self-digestion: molecular mechanisms and biological functions of autophagy. *Dev Cell* 6: 463–477
- Majno G, Joris I (1995) Apoptosis, oncosis, and necrosis. An overview of cell death. *Am J Pathol* 146: 3–15
- Marcu MG, Schulte TW, Neckers L (2000) Novobiocin and related coumarins and depletion of heat shock protein 90-dependent signaling proteins. *J Natl Cancer Inst* 92: 242–248
- Matsui H, Asou H, Inaba T (2007) Cytokines direct the regulation of Bim mRNA stability by heat-shock cognate protein 70. *Mol Cell* 25: 99–112
- Mei Y, Xie C, Xie W, Tian X, Li M, Wu M (2007) Noxa/Mcl-1 balance regulates susceptibility of cells to camptothecin-induced apoptosis. *Neoplasia* 9: 871–881
- Melo JV, Brito-Babapulle V, Feroni L, Robinson DS, Luzzatto L, Catovsky D (1986) Two new cell lines from B-prolymphocytic leukaemia: characterization by morphology, immunological markers, karyotype and Ig gene rearrangement. *Int J Cancer* 38: 531–538
- Mimnaugh EG, Xu W, Vos M, Yuan X, Isaacs JS, Bisht KS, Gius D, Neckers L (2004) Simultaneous inhibition of hsp 90 and the proteasome promotes protein ubiquitination, causes endoplasmic reticulum-derived cytosolic vacuolization, and enhances antitumor activity. *Mol Cancer Ther* 3: 551–566
- Mimnaugh EG, Xu W, Vos M, Yuan X, Neckers L (2006) Endoplasmic reticulum vacuolization and valosin-containing protein relocalization result from simultaneous hsp90 inhibition by geldanamycin and proteasome inhibition by velcade. *Mol Cancer Res* 4: 667–681
- Muller P, Hrstka R, Coomber D, Lane DP, Vojtesek B (2008) Chaperone-dependent stabilization and degradation of p53 mutants. *Oncogene* 27: 3371–3383
- Oda E, Ohki R, Murasawa H, Nemoto J, Shibue T, Yamashita T, Tokino T, Taniguchi T, Tanaka N (2000) Noxa, a BH3-only member of the Bcl-2 family and candidate mediator of p53-induced apoptosis. *Science* 288: 1053–1058
- Pérez-Galán P, Roué G, Villamor N, Campo E, Colomer D (2006) The proteasome inhibitor bortezomib induces apoptosis in mantle-cell lymphoma through generation of ROS and Noxa activation independent of p53 status. *Blood* 107: 257–264
- Pratt WB, Toft DO (2003) Regulation of signaling protein function and trafficking by the hsp90/hsp70-based chaperone machinery. *Exp Biol Med* 228: 111–133
- Quintanilla-Martinez L, Davies-Hill T, Fend F, Calzada-Wack J, Sorbara L, Campo E, Jaffe ES, Raffeld M (2003) Sequestration of p27Kip1 protein by cyclin D1 in typical and blastic variants of mantle cell lymphoma (MCL): implications for pathogenesis. *Blood* 101: 3181–3187
- Raynaud SD, Bekri S, Leroux D, Grosgeorge J, Klein B, Bastard C, Gaudray P, Simon MP (1993) Expanded range of 11q13 breakpoints with differing patterns of cyclin D1 expression in B-cell malignancies. *Genes Chromosomes Cancer* 8: 80–87
- Robles AI, Wright MH, Gandhi B, Feis SS, Hanigan CL, Wiestner A, Varticovski L (2006) Schedule-dependent synergy between the heat shock protein 90 inhibitor 17-(dimethylaminoethylamino)-17-demethoxygeldanamycin and doxorubicin restores apoptosis to p53-mutant lymphoma cell lines. *Clin Cancer Res* 12: 6547–6556
- Sampath J, Sun D, Kidd VJ, Grenet J, Gandhi A, Shapiro LH, Wang Q, Zambetti GP, Schuetz JD (2006) Mutant p53 cooperates with ETS and selectively up-regulates human MDR1 not MRP1. *Clin Cancer Res* 12: 3459–3469
- Samraj AK, Stroth C, Fischer U, Schulze-Osthoff K (2006) The tyrosine kinase Lck is a positive regulator of the mitochondrial apoptosis pathway by controlling Bak expression. *Oncogene* 25: 186–197

- Shen S, Zhang P, Lovchik MA, Li Y, Tang L, Chen Z, Zeng R, Ma D, Yuan J, Yu Q (2009) Cyclodepsipeptide toxin promotes the degradation of Hsp90 client proteins through chaperone-mediated autophagy. *J Cell Biol* **185**: 629–639
- Sherr CJ, Roberts JM (1999) CDK inhibitors: positive and negative regulators of G₁-phase progression. *Genes Dev* **13**: 1501–1512
- Smit LA, Hallaert DY, Spijker R, de Goeij B, Jaspers A, Kater AP, van Oers MH, van Noesel CJ, Eldering E (2007) Differential Noxa/Mcl-1 balance in peripheral versus lymph node chronic lymphocytic leukemia cells correlates with survival capacity. *Blood* **109**: 1660–1668
- Tse AN, Sheikh TN, Alan H, Chou TC, Schwartz GK (2009) 90-kDa heat shock protein inhibition abrogates the topoisomerase I poison-induced G2/M checkpoint in p53-null tumor cells by depleting Chk1 and Wee1. *Mol Pharmacol* **75**: 124–133
- Tsujimoto Y, Shimizu S (2005) Another way to die: autophagic programmed cell death. *Cell Death Differ* **12**: 1528–1534
- Van Cruchten S, Van Den Broeck W (2002) Morphological and biochemical aspects of apoptosis, oncosis and necrosis. *Anat Histol Embryol* **31**: 214–223
- Warr MR, Shore GC (2008) Unique biology of Mcl-1: therapeutic opportunities in cancer. *Curr Mol Med* **8**: 138–147
- Willis SN, Chen L, Dewson G, Wei A, Naik E, Fletcher JI, Adams JM, Huang DC (2005) Proapoptotic Bak is sequestered by Mcl-1 and Bcl-xL, but not Bcl-2, until displaced by BH3-only proteins. *Genes Dev* **19**: 1294–1305
- Yan W, Chen X (2009) Identification of GRO1 as a critical determinant for mutant p53 gain of function. *J Biol Chem* **284**: 12178–12187
- Zhang R, Luo D, Miao R, Bai L, Ge Q, Sessa WC, Min W (2005) Hsp90-Akt phosphorylates ASK1 and inhibits ASK1-mediated apoptosis. *Oncogene* **24**: 3954–3963
- Zhang Y, Wang JS, Chen LL, Cheng XK, Heng FY, Wu NH, Shen YF (2004) Repression of hsp90beta gene by p53 in UV irradiation-induced apoptosis of Jurkat cells. *J Biol Chem* **279**: 42545–42551